crv4, a mouse model for human ataxia associated with kyphoscoliosis caused by an mRNA splicing mutation of the metabotropic glutamate receptor 1 (*Grm1*)

VALERIO CONTI[1,2], ASADOLLAH AGHAIE[3], MICHELE CILLI[4], NATALIA MARTIN[3], GIANLUCA CARIDI[5], LUCA MUSANTE[2,5], GIOVANNI CANDIANO[5], MAURA CASTAGNA[6], ALFONSO FAIREN[7], ROBERTO RAVAZZOLO[1,8], JEAN-LOUIS GUENET[3] and ALDAMARIA PULITI[1,8]

[1]Laboratory of Molecular Genetics, and [2]Renal Child Foundation, G. Gaslini Institute, Genova, Italy; [3]Unité de Génétique fonctionnelle de la Souris, Institut Pasteur, Paris, France; [4]Animal Models Facility, Istituto Nazionale per la Ricerca sul Cancro, Genova; [5]Laboratory on Pathophysiology of Uremia, G. Gaslini Institute, Genova; [6]Laboratorio di Anatomia Patologica, Department of Surgery, University of Pisa, Pisa, Italy; [7]Instituto de Neurociencias, CSIC and Universidad Miguel Hernández, San Juan de Alicante, Spain; [8]Department of Pediatrics and CEBR, University of Genova, Italy

Received March 29, 2006; Accepted May 26, 2006

Abstract. We describe a novel spontaneous autosomal recessive mutation, *cervelet-4* (*crv4*), which arose in a BALB/c strain. Mice homozygous for the mutation exhibit principally a reduced body size, a congenital neurological phenotype characterized by ataxic gait and intention tremor, with no gross anomalies observed in brain or cerebellum, and skeletal anomalies. Using linkage analysis, we mapped the *crv4* locus to the proximal region of chromosome 10, at the location of the *Grm1* gene. Genetic complementation crosses between *crv4* and *Grm1* KO mice confirmed that *crv4* is a new allele of *Grm1*. Molecular analysis of the *Grm1* gene in mutant mice revealed the insertion of a 190-bp LTR fragment in intron 4. Our results also indicated that the presence of the LTR fragment caused the disruption of the *Grm1* normal splicing process and complete absence of the wild-type protein. *crv4* is an interesting model to extend the study of *Grm1* function and the pathological effects of *Grm1* deficiency *in vivo*.

Introduction

Glutamate is the major excitatory neurotransmitter in the mammalian central nervous system (CNS) and plays an important role in a number of central nervous system functions (1). Metabotropic glutamate receptors (mGluRs), one of the two broad categories in which glutamate receptors are classified, are mainly involved in the regulation of synaptic plasticity, such as long-term potentiation and long-term depression, which are thought to be models of learning and memory (2). mGluRs consist of at least eight subtypes that regulate a variety of intracellular signalling systems via activation of GTP-binding proteins (3). Glutamate receptor metabotropic 1 (*Grm1*) is present in a number of key CNS structures including the hippocampus, cortex, thalamus and cerebellum and the involvement of this receptor in a variety of disorders including mainly ataxia, epilepsy, ischemia, pain and neurodegenerative diseases is beginning to emerge (1). In general, the biological cause of these disorders can be intrinsic defects of structure or function of cerebellum or its connections (4). An invaluable resource to aid the understanding of the processes underlying these defects are mouse neurological mutations.

In the present study we describe a spontaneous mouse mutation, *cervelet-4* (*crv4*), that occurred in the *Grm1* gene and results from the insertion of a retrotransposon LTR fragment in an intron. This insertion generates abnormal splicing of the gene with occurrence of a premature 'in-frame' stop codon. As a final consequence, the wild-type *Grm1* protein is not present in *crv4*/*crv4* mutants thus the mutant mouse is a model of *Grm1*-deficiency, the peculiarity of which will be useful to further understand *Grm1*'s function and its involvement in human disease.

Materials and methods

Mice. The *crv4* mutation occurred spontaneously in the BALB/c/Pas inbred strain maintained at the Institut Pasteur and was transferred into the Animal Models Facility, Istituto Nazionale per la Ricerca sul Cancro in Genova. The MAI/Pas strain used for mapping of the mutation, is a new inbred from the Institut Pasteur that is derived from wild specimens of the *Mus m. musculus* subspecies. *Grm1* KO mice were obtained from GlaxoSmithKline (5) and were maintained in the Servicio

Correspondence to: Professor Roberto Ravazzolo, Laboratory of Molecular Genetics, G. Gaslini Institute, Largo G. Gaslini 5, 16148 Genova, Italy
E-mail: rravazzo@unige.it

Key words: ataxia, kyphoscoliosis, *Grm1*, retrotransposon insertion, additional exon, splicing error

de Experimentación Animal at the Universidad Miguel Hernández of San Juan de Alicante.

Footprint analyses. Footprint analyses were performed according to a previously described protocol (6). In brief, mice were trained to cross an illuminated alley (5 cm wide, 80 cm long) and to go straight to a dark box located at the end of the alley. Their footpads were then coated with a non-toxic, water-based paint, and the floor of the alley was covered with white paper. This test was repeated three times and the footprints were scanned in order to evaluate the deviation of foot placement.

X-ray analysis. Mice were briefly narcotized to facilitate radiography, performed by using a LORAD M-IV system. For comparative purposes, identical radiation energy and photographic exposures were used to prepare radiographs of *crv4*/*crv4* and sex- and age-matched control mice.

Genetic mapping. Chromosomal location of the *crv4* locus was achieved by genotyping a large set of DNA samples prepared from (BALB/c x MAI)F2 mice, homozygous for the *crv4* allele (*crv4*/*crv4*), with a collection of microsatellite markers, spaced at <20 cM and known to be polymorphic between the two parental strains. PCR reactions were carried out using a standard protocol (7) on 100 ng of tail DNA.

Grm1 genomic PCR. All coding sequences and exon-intron boundaries of the *Grm1* gene were amplified by using primers designed on the sequence of the flanking exons. Exons 2, and 8 and the last exon containing the polyadenylation site, which are 1018, 931 and 1144 bp long respectively, were amplified in 2 overlapping fragments. Primers genlongF (5'-CAATTCC ATAATGCTCATAATGCATCC-3') and genlongR (5'-AAT ACTTTCATGTGTAGACCTTAGTCCAA-3') designed on the intron 4 sequence, were used to specifically amplify the inserted fragment. All PCR amplifications were performed by using the HOT FIREpol DNA polymerase I (Solis Biodyne), with 50˚C annealing and a final extension of 72˚C for 10 min. PCR products were analysed on 1% agarose gel (SeaKem LE agarose, FMC bioproducts) and visualized by classical ethidium bromide staining.

Grm1 RT-PCR. Total RNA was extracted from normal and mutant cerebella by using Trizol reagent (Gibco) according to the manufacturer's protocol. For RT-PCR reactions, 1 μg of total RNA was used to synthetize the first-strand cDNA by using the ImProm-II™ reverse transcription system (Promega), according to the manufacturer's protocol. The 4237-bp long *Grm1*a isoform was amplified by using the Expand long template PCR system (Roche), with the primers *Grm1*F1 (5'-AGCCTTGCACCGTCTGAT-3') and *Grm1*R1 (5'-ACTC CTTGGCATCTCTGG-3'). The *Grm1* cDNA was amplified with the aim of sequencing by using the Expand High Fidelity PCR system (Roche) and the following set of overlapping primers: *Grm1*F1 (5'-AGCCTTGCACCGTCTGAT-3') and *Grm1*R2 (5'-CCTGCCAGCAGTACTTTT-3'); *Grm1*F2 (5'-TTCCCAATGATCTTTTTG-3') and *Grm1*R3 (5'-TGGGAT GTCGAACAGCTG-3'); *Grm1*F3 (5'-TACCCCCAGGCAG GACTAAG-3') and *Grm1*R4 (5'-GAGTGAGAACTCTCCC AC-3'); *Grm1*F4 (5'-ATGACAGTGCGGGGGTTA-3') and *Grm1*R5 (5'-TCCAGACACTCAACAAA-3').

Sequencing. Both genomic and RT-PCR products were purified with the ExoSap-IT enzyme (USB) then sequenced on both strands using BIG DYE dideoxy-terminator chemistry (Applied Biosystem) on an ABI 3100 DNA sequencer (Applied Biosystem).

Northern blot analysis. Twenty-five micrograms of total RNA isolated from cerebellum was electrophoresed in a 1.0% agarose/formaldehyde gel. The gel was blotted onto Hybond-N nylon membrane (Amersham), probed with a 969-bp RT-PCR product (Genbank AF320126, bp 3100 to 4069) of mouse *Grm1*, and reprobed with a 1290-bp RT-PCR product specific for the mouse ß-actin gene (b-act F, 5'-GCATTGTTACCAA CTGGGAC-3'; R, 5'- CCAGAGCAGTAATCTCCTTC-3').

Histological analyses and immunohistochemistry. Animals were deeply anaesthetized with xylazine and ketamine and transcardially perfused with phosphate buffered saline (PBS, pH 7.4), followed by 4% paraformaldehyde (PFA) in 0.1 M, pH 7.4 PBS. Organs were then removed and either embedded in paraffin wax or, after sucrose cryoprotection, frozen in OCT (Tissue Tec, Sakura) for the histological analyses. Sagittal and coronal sections, 5 μm each, obtained from paraffin embedded tissues, were stained with Haematoxylin and Eosin or Nissl staining. For immunohistochemistry, both paraffin embedded and frozen brains were sectioned in coronal plane at 5 μm (paraffin embedded) or 20 μm (frozen) thickness. Sections were pre-incubated (30 min) in 10% donkey serum in PBS, rinsed in PBS and incubated overnight at 4˚C with 5 μg/ml polyclonal anti-*Grm1*a antibody (Upstate Biotechnology). Sections were rinsed in PBS and incubated for 30 min with the secondary antibody (Donkey anti-rabbit IgG B, Santa Cruz biotechnology). After two rinses in PBS, the sections were processed for 30 min with the biotin-streptavidin-peroxidase complex (Vectastain ABC Elite kit, Vector) according to the manufacturer's instructions. Sections were then incubated in DAB substrate kit for peroxidase (Vector) and treated with H_2O_2 for 1-6 min.

Western blotting. Western blotting was performed according to established protocols (8,9) with some modifications. In brief, cerebella were homogenized in buffer A (5 mM Tris pH 7.2, 2 mM EDTA, 10 mM iodoacetamide and protease inhibitors), and then centrifuged at 30,000 x g for 30 min at 4˚C to collect a crude membrane pellet. The pellet was re-suspended in buffer B (20 mM Tris-HCl pH 6.8, 150 mM NaCl, 10 mM EDTA, 1 mM EGTA, 1% Triton X-100, 10 mM iodoacetamide and protease inhibitors mixture). Protein concentration was determined by the Bradford method (Bio-Rad) and samples were separated on 5% gel by SDS-PAGE. Proteins were electroblotted and protein transfer was monitored by Ponceau Red S staining. Membranes were then incubated with either the anti-*Grm1*a monoclonal antibody (BD Biosciences) at a dilution of 1:2500, or the polyclonal anti-*Grm1*a antibody (Upstate Biotechnology). The *Grm1* bands were detected with an enhanced chemiluminescence system Versa-Doc 4000 (Bio-Rad).

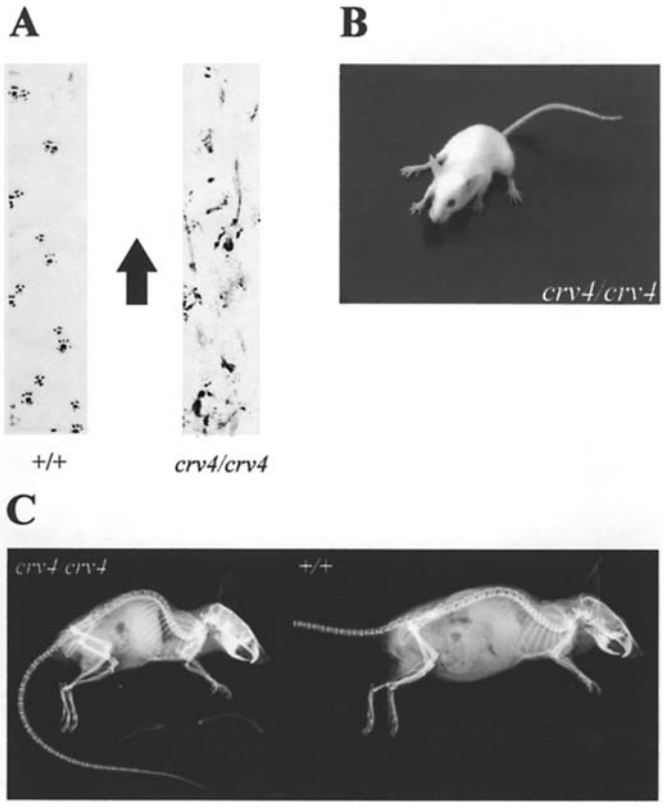

Figure 1. *crv4* anomalous gait and posture. (A) Footprint analysis. *crv4*/*crv4* mice walked with a severe wide base rolling motion from side to side and their feet tended to sweep along the floor; as a consequence their gait was severely altered with respect to control mice. (B) *crv4*/*crv4* mice seemed also to have a mild spasticity of the posterior limbs. (C) X-ray radiography of 10-month-old *crv4*/*crv4* and control (+/+) mice. The *crv4*/*crv4* mouse exhibited thoracic kyphoscoliosis. Due to curvature of the spinal column at the shoulder level, the thoracic region in the *crv4*/*crv4* mouse protruded prominently.

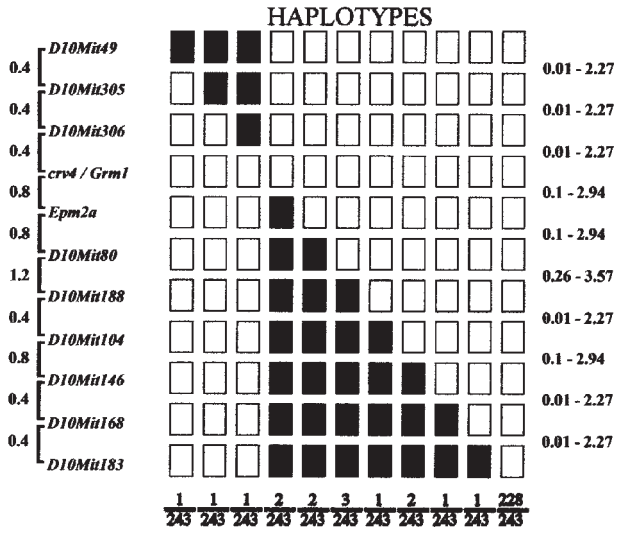

Figure 2. Haplotypes diagram of markers used for mapping the *crv*4 locus. Distribution of the different haplotypes among 121 offspring of an intercross between strain BALB/c, where the mutant allele appeared, and strain MAI/Pas. All mice but one in this diagram were homozygous for the mutant allele *crv4* while one unaffected mouse progeny, tested as +/*crv4*, was added (243 meiosis in total). Filled rectangles, MAI/Pas alleles; white rectangles, BALB/c alleles. The molecular markers used for genotyping are on the left. The intervals between any two markers are provided with confidence intervals at the 5% risk level. Genotyping of these haplotypes indicates that the locus for *crv4* is within a 1.2-cM interval, flanked by markers *D10Mit306* and *Epm2a*, which is equivalent to 2 Mbp of mouse DNA. Marker order and distances established from our cross are in perfect fit with the sequence data available.

Sequence analysis of the LTR-fragment. The sequence of *Grm1* intron 4, including *crv4* genomic insertion, was compared to wild-type sequence by using the BLAST program (http://www.ncbi.nlm.nih.gov/BLAST/). Open Reading Frame Finder software (http://www.ncbi.nlm.nih.gov/gorf/orfig.cgi) was used to predict the translation of the mutated protein. Alternative Splicing Workbench (http://www.ebi.ac.uk/asd-srv/wb.cgi) and SpliceView (http://l25.itba.mi.cnr.it/~webgene/wwwspliceview.html) programs were used to recognize splicing acceptor and donor sites, polypyrimidine tracts (PPT) and branchpoint (BP) sites in the upstream intronic sequence of the new inserted exon. ESEfinder (http://rulai.cshl.edu/tools/ESE/) and ACESCAN2 (http://genes.mit.edu/acescan2/) programs were used to evaluate the presence of exonic splicing enhancers (ESE) or exonic splicing silencers (ESS) in the new inserted exon.

Results

Phenotype of the crv4 mutant. While +/*crv4* heterozygous are normal, mice of both sexes homozygous for the new mutation *crv4* (*crv4*/*crv4*) are viable but exhibit, from birth, a reduction in size by roughly 1/3. Homozygous females show very reduced fertility while males seem to be sterile. Anomalous posture, whole body tremor during movement and ataxic gait are the main features which became clearly evident when the mice started walking. Footprint analysis indicated that mutant mice walked with a severe wide base rolling motion from side to side, they could not walk along a straight line and their feet tended to sweep along the floor. The impairment of motor coordination in *crv4*/*crv4* mice also seemed to be associated to a mild spasticity of the posterior limbs (Fig. 1A and B). The morphology of the cerebellum appeared unaffected by the *crv4* mutation, as shown in hematoxylin and eosin- and Nissl-stained material. Purkinje cell number, size and distribution were also normal. No gross anomalies were found in the hippocampus or elsewhere. *crv4*/*crv4* mice exhibited an ocular anomaly, either unilateral or bilateral, with their eyes being more closed than in the control. Eye section revealed no gross anomalies. Twelve *crv4*/*crv4* mice (6 females and 6 males), 6/8 months old and BALB/c controls were sacrificed and investigated for the presence of additional phenotype anomalies. The following features were frequently observed: an increased amount of interscapular brown fat, which was nearly doubled in females compared with control mice; and a kyphoscoliotic defect, particularly evident in females, upon necropsy analysis and by alizarin red/alcian blue skeletal staining and X-ray analysis in three additional affected animals (Fig. 1C).

Genetic mapping of the mouse crv4 locus. Genetic mapping was performed in two steps on a total sample of 121 *crv4*/*crv4* F2 mice. An initial chromosomal assignment using 21 DNA samples of affected animals suggested linkage of the *crv4* locus with several markers of chromosome 10. High resolution

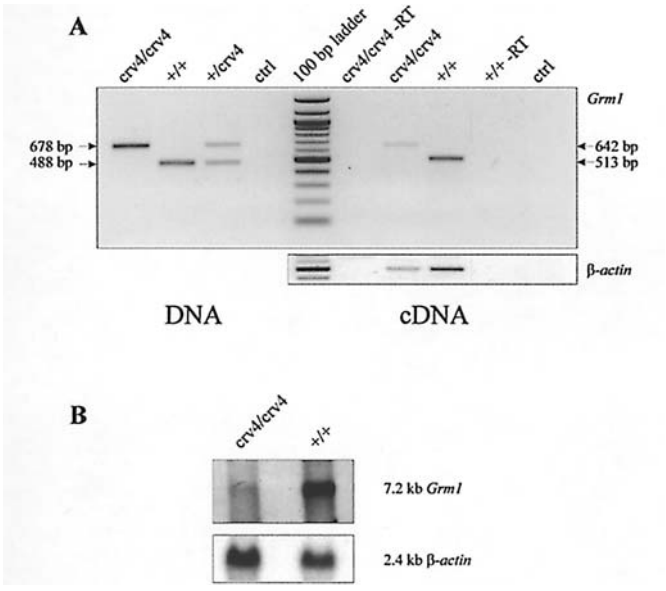

Figure 3. (A) Genomic and RT-PCR analysis of *crv4* mutants. In both cases the upper bands represent the inserted sequence, the lower bands represent the wild-type sequence. cDNA insertion is 139 bp long, while the entire insertion is 190 bp long at genomic level. (B) Northern blot analysis of *Grm1* expression in wild-type and *crv4*/*crv4* mice. In *crv4*/*crv4* mice, the *Grm1* main transcript is detectable at very low levels. As a control for RNA quantity, the same blot was reprobed with a ß-actin cDNA fragment.

mapping in the critical region with all 121 samples indicated that the *crv4* locus maps within the 1.2-cM interval flanked by markers *D10Mit306* and *Epm2a* (Fig. 2). In this interval, the *Grm1* gene appeared as a strong candidate because of striking similarities between the pathophysiological features reported for the *Grm1* knockout (*Grm1*$^{-/-}$) and our *crv4* mutant allele (5,10,11).

crv4 is a new allele at the Grm1 locus. Heterozygous +/*crv4* mice were crossed with *Grm1*$^{+/-}$ mice, in which one copy of the *Grm1* gene was disrupted by the insertion of a *lac*Z/neo^{r} expression unit in the domain encoding the second intracellular loop of the seven transmembrane domain of the molecule (5). Both *crv4* and *Grm1* are null mutations. As expected for recessive mutations, on the average 1/4 of the F_1 progeny obtained from this cross exhibited the neurological phenotype characteristic of *crv4*, confirming that *crv4* is indeed a new null allele at the *Grm1* locus.

Molecular characterization of the crv4 mutation. To assess whether *crv4* mice have any structural change in the coding sequence of the *Grm1* gene, we checked the sequence of all known exons of the *Grm1* gene in *crv4*/*crv4* mutant mice as well as the sequence of the regions flanking the splicing sites by amplifying genomic DNA fragments encompassing the whole region. We found no mutation. We then decided to analyse the *Grm1* cDNA derived from the cerebellum of the *crv4*/*crv4* mutant mice and control. We observed an amplification product of the expected size, corresponding to the *Grm1*a isoform (12) in the control mice, but the unique product amplified from *crv4*/*crv4* mice cerebellum cDNA showed an increased size leading us to suspect that an insertion might have occurred in the genomic sequence leading to abnormal splicing. To test this hypothesis and identify the suspected insertion site at the RNA level, a series of overlapping RT-PCR followed by cDNA sequencing were performed and a 139-bp insertion between exons 4 and 5 was found corresponding to an inserted DNA fragment of 190 bp at the genomic level (Fig. 3). BLAST analysis indicated that the inserted segment shares 94% homology with 5' LTR and primer binding sequences of the *Mus m. domesticus* endogenous retroviral element MuERV-L (Y12713) but lacks the other specific MuERV-L features. The LTR fragment was inserted in the same orientation as the *Grm1* gene, and interferes with the normal splicing of the gene by inducing the transcription of an additional exon composed of 23 bp from intron 4 and 116 bp from the LTR-fragment, with an in-frame stop codon (Fig. 4A). Since no evidence of wild-type mRNA presence was obtained by RT-PCR, with either full-length cDNA or with exon 4 and 5 specific primers at different PCR conditions, we assumed that the only transcribed mRNA was the mutated one and, as a consequence, that a wild-type protein was not translated from the mutant transcript. Northern blot analysis of RNA from wild-type and mutant mice (Fig. 3) demonstrated the presence of a *Grm1* specific band although at very low levels.

We investigated the 500 bp intronic sequence encompassing the insertion site for the presence of specific features, which could have favoured the insertion and the preferential expression of the mutant spliced mRNA. The insertion interrupts a 72-bp long SINE sequence of the ID4 family (MUSID4) causing a rearrangement of 18 SINE specific bp (Fig. 4B).

Furthermore, the inserted LTR-fragment sequence introduces a donor 'GT' site, at least 7 murine exonic splicing enhancers (ESEs) and a sequence homologous to a human known silencer (Fig. 4B). An acceptor splice site, polypyrimidine tracts (PPTs) and a branchpoint site, necessary for correct splicing, were identified in a range of 34 bp upstream of the new exon.

Expression of Grm1 protein in crv4 mice. Western blot and immunohistochemistry analyses showed absence of the wild-type *Grm1* protein in the cerebellum, consistent with the absence of wild-type mRNA. Western blot and immunohistochemistry analyses were performed by using antibodies that recognize the *Grm1*a isoform. In Western blotting, monoclonal and polyclonal anti-Grm1 antibodies recognized an ~140-kDa band corresponding to receptor monomers, and a higher molecular weight band, which may correspond to receptor dimers (9,13), in control mice, whereas no protein expression was found in cerebellar extract from *crv4*/*crv4* mice (Fig. 5A). In the cerebellum, *Grm1* is expressed by Purkinje cells perisinaptically with respect to parallel fiber-Purkinje cell synapses. Golgi, basket, stellate and Lugaro cells also express *Grm1* (14). Immunohistochemistry performed on frozen and paraffin embedded cerebellar sections with a polyclonal antibody raised against the C-terminal region of *Grm1*a demonstrated the absence of wild-type *Grm1* protein in all layers of the cerebellum (Fig. 5B).

Discussion

In this paper we report the genetic and phenotypic analysis of *cervelet-4* (*crv4*), a new spontaneous mouse model that exhibits

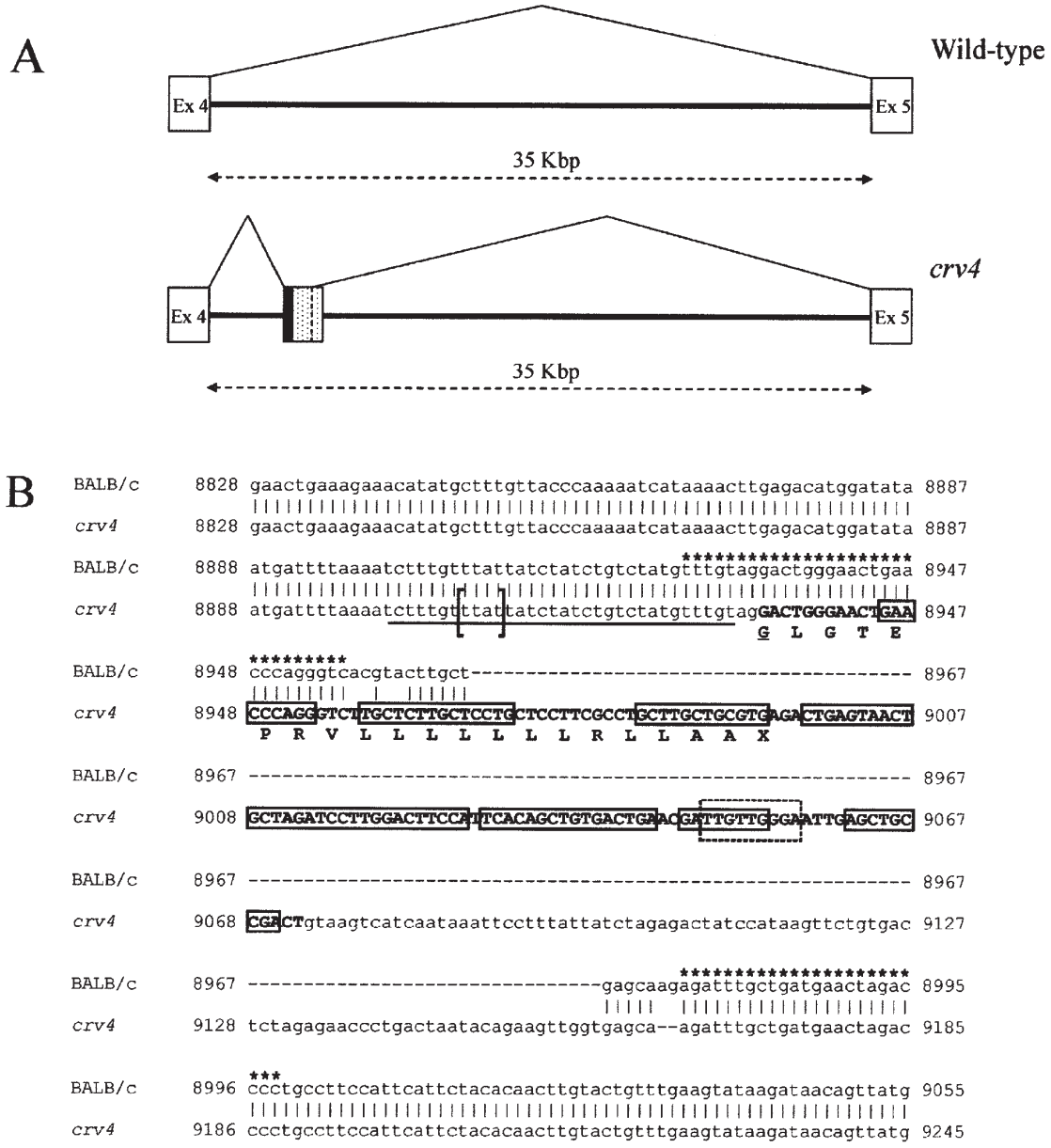

Figure 4. Sequence analysis of *Grm1* intron 4. (A) Genomic structure in-between exons 4 and 5 of wild-type and *crv4* mice. Wild-type and possible aberrant splicing mechanisms are indicated as thin lines. Exons 4 and 5 are also indicated. Dotted box, the LTR fragment insertion, the spliced part of the LTR is delimited by the vertical outlined line; black box, the part of intron 4 that is spliced in crv4. (B) Nucleotide sequence comparison of wild-type and *crv4* mice. The alignment between wild-type and *crv4* sequences is indicated. Uppercase bold letters represent the new inserted exon, the relative translation is also indicated. The polypyrimidine tract is underlined, and the branchpoint tract is indicated by squared parenthesis. Open boxes, ESE sequences; outlined box, the ESS sequence; stars, the position of SINE specific regions.

a recessive phenotype, characterized mostly by congenital ataxia and intention tremor. This ataxic mouse, in which the *Grm1* gene carries an insertion affecting the normal splicing process with consequent loss of the wild-type protein, is of particular interest both as a model for the identification of molecular mechanisms of ataxia pathogenesis and because of the peculiarity and originality of the mutation mechanism.

The *crv4* mutation is the consequence of the insertion of a 190-bp retrotransposon LTR fragment, homologous to the MuERV-L element, which occurred in intron 4 of the *Grm1* gene. The insertion caused the introduction of an extra exon and an in-frame stop codon in the *Grm1* mRNA sequence. Since no wild-type *Grm1* RNA was detected by RT-PCR, we concluded that the additional exon is constitutively spliced in the mature mRNA while the normal splicing is disrupted. Integration of retroviruses or retrotransposons into the host chromosome have already been reported to result in the inhibition or activation of the expression of targeted genes. The mouse mutations *dilute* (*Myo5a* - Chr 9) (15) and *hairless* (*Hr* - Chr 14) (16) are examples of such spontaneous mutations caused by retroviral insertion. In these mutants, the insertion, which occurred in introns, was associated to a reduced or aberrant expression of the endogenous gene leading to *dilute* and *hairless* phenotypes respectively. Interestingly, in these models the proviral excision through homologous recombination between the two Long Terminal Repeats (LTR), leaving a 'solo LTR' in the host chromosome, was associated to a reversion of the phenotype to normal, thus indicating that

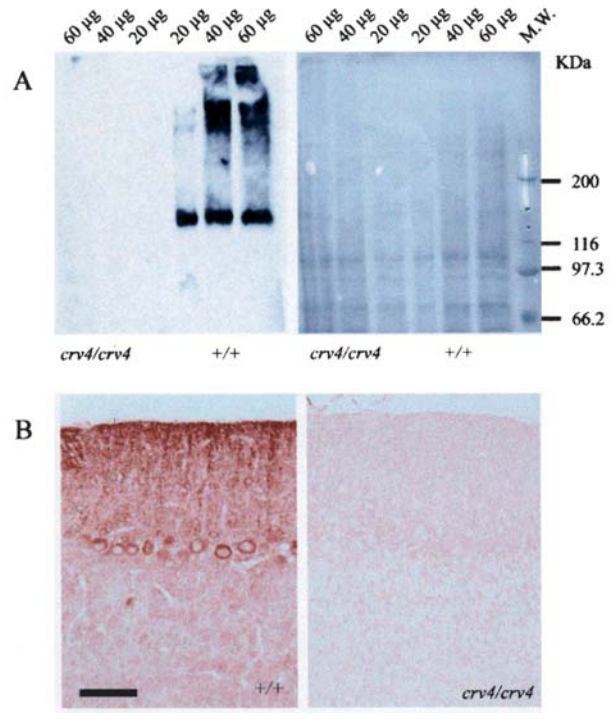

Figure 5. *Grm1* expression in wild-type and *crv4* mice cerebella. (A) Western blot analyses performed with antibodies that recognise the C-terminal domain of *Grm1* protein indicate no *Grm1* expression in cerebellar membrane extracts from *crv4/crv4* mice. (B) No staining was observed in any cerebellar structure of *crv4/crv4* mice by immunohistochemistry, compared to normal control mice. Bar, 50 μm.

a 'solo LTR' has no mutagenic effect. In the case of the *dilute* and *hairless* genes, the presence of the intronic 'solo LTR' allowed the expression not only of an aberrant, but also a normal mRNA form, sufficient to revert the anomalous phenotype (17); this is in agreement with the well-known mechanism by which homologous recombination between two LTRs has led to the production of 'solo LTRs' that are scattered randomly throughout the genome with no consequence on phenotype (18). To the best of our knowledge, only one case in which the insertion of a 'solo LTR' in an intronic region was associated with a pathological phenotype has been reported so far (19). In that case, the insertion of a 520-bp 'solo LTR' (conserving all the classical LTR features) in intron 22 of the *mdr-3* gene caused disruption of the normal splicing process. In all other reported cases, the presence of intronic 'solo LTRs' seems to be associated to normal phenotype (19). Thus, the *crv4* inserted sequence is the smallest LTR-fragment reported to be inserted in an intronic region and to be associated with an aberrant phenotype in mice. To elucidate why the *crv4* LTR-fragment, which is only 190 bp long, is able to induce an aberrant splicing of the *Grm1* gene, we analysed the inserted sequence and its flanking intronic regions with softwares that can recognize splicing regulation sequences. Accurate and efficient pre-mRNA splicing is essential to ensure correct gene expression and specific consensus sequences (5' acceptor splice site, branch site and 3' donor splice site) are found at virtually all exon-intron joints (20). Interestingly, acceptor splicing sites were found in the analysed region in both *crv4* and wild-type mice. On the contrary, no donor splice sites were identified in approximately 500 bp encompassing the intronic site of insertion in the wild type, while several donor splice sites were predicted in the mutant sequence, among which is the effective *crv4* spliced donor site. In addition, branch point (BP) and Polypyrimidine tracts (PPTs) were also found in the first 34 bp flanking the acceptor site, a distance compatible with that present in normal spliced exons (21). Additional regulatory *cis*-elements are exonic splicing enhancers (ESEs) and exonic splicing silencers (ESSs). These sequences are known to regulate splicing positively (ESEs) or negatively (ESSs) by the stimulation or inhibition of splicing machinery recruitment (22,23). ESEs, in particular, may be present in most, if not all, exons including constitutive ones (exons always included in the mature mRNA, even in different mRNA isoforms) (24). In the new exon generated in *crv4* mRNA, several putative ESEs and only one ESS sequence, in part overlapping one of the predicted ESEs, were predicted (Fig. 4B). It is known that ESEs, when present together, act in a dominant manner over adjacent ESSs (25). Consistent with the absence of detectable wild-type *Grm1* mRNA in *crv4* mutants, and because of the high ratio between the number of predicted ESEs and ESSs, we hypothesised that the new additional exon was spliced in the mRNA as a constitutive one. In order to evidence the presence of specific features, such as repeats containing sequences, which could have favoured the insertion of the identified fragment, the intron 4 sequence of the *Grm1* gene was analyzed. The results showed that the LTR-fragment is localized in the central region of a SINE element. SINEs are small elements, usually 100-400 bp in length, which lack a protein-coding sequence and therefore rely on other elements for their retrotransposition (18). It has been reported that human *Alus*, and B1 and B2 rodent SINE sequences can mediate the integration of flanked sequences by homologous or illegitimate recombination (26,27). In addition, it has been reported that LTR containing retrotransposons can contain 'hot spots' for SINE insertion (28). Consistent with these observations, we hypothesise that such an insertion could have been mediated by a two-step process in which both the SINE and the LTR retrotransposon may have played a role. Overall, the peculiarity of the *crv4* mutation underlines the importance of mutations leading to gene function disruption through mechanisms different from simple variations in coding sequences and involving splicing regulatory sequences located far from coding regions.

Expression of the *Grm1* mRNA was investigated by two techniques. Northern blot analysis detected in *crv4/crv4* mice a *Grm1* specific band at a very low level. The size of the detected band appeared to be approximately the same as in the control, which was expected since the difference between the wild type and the mutated form consists only in 139 bp, a difference not detectable by Northern blot analysis. Thus, by Northern blot analysis we were not able to determine if the observed band resulted from an aberrant or from a residual normal *Grm1* RNA splicing process. On the contrary RT-PCR, which could discriminate the two differently spliced forms, indicated the presence of the mutation as a unique expressed mRNA form. The Northern blot and RT-PCR results together indicate that only the mutant form was present in *crv4* homozygous mice although at a very low level. It is noteworthy that mRNAs containing premature-termination codons as a

result of mutations are hampered to be translated in truncated and potentially harmful proteins by a cell surveillance pathway known as nonsense-mediated mRNA decay (NMD) (29). It is thus possible that the low level of mRNA detected in affected mice, reflecting its very low stability, could result from an NMD mechanism. In case some mutated mRNA molecules escape the surveillance system, a short polypeptide could be produced.

The predicted *crv4* protein, shorter than the wild type (415 aminoacids instead of 1,199) retains 396 aa at the N-terminal to which 19 aa derived from the intronic and inserted LTR-fragment are added (Fig. 4B). Since the seven transmembrane domains of the *Grm1* protein start from aminoacid 594 (2), we hypothesise that the mutated protein loses its membrane anchoring and, if not degraded, can reach the plasmatic membrane and be secreted. Previous reports provide some support to the hypothesis that naturally secreted isoforms of the *Grm1* protein exist. A short form of *Grm1* mRNA (E55) was detected by RT-PCR in mice although the presence of its translated product was not reported. The predicted protein was 321 aa long, containing only the extracellular domain, which could possibly be secreted (30). In addition, Selkirk and collaborators obtained *in vitro* the synthesis of a secreted polypeptide by transfecting a Chinese hamster ovary cell line with a construct containing residues 1-592 of the human *Grm1* N-terminal domain. They demonstrated that this secreted protein maintains a pharmacological profile similar to that of the native receptor and the ability to bind glutamate (31).

Unfortunately, the unavailability of *Grm1* antibodies specific for the N-terminal part of the protein makes the detection of the *crv4* truncated protein difficult to achieve. It is worth noting that, if the truncated protein was secreted, it could have great implications in the extracellular glutamate balance, probably influencing the interactions of glutamate with other receptors. The potential presence of a secreted truncated protein represents a unique feature of *crv4* mice, compared with the previously described *Grm1* null mice (5,10,11). This could be the reason why additional anomalies, such as kyphoscoliosis, which have not been described in *Grm1* null mice (5,10,11), have been observed in *crv4*/*crv4* mice. On the contrary, the eye defect observed in *crv4*/*crv4* mice may be a consequence of the impairment of the conditioned eyeblink response which was already observed in the *Grm1* KO mice by electrophysiological tests (11). Recently, a new mouse mutant carrying a null mutation of the *Grm1* gene in a 129P2/OlaHsd-C57BL/6 genetic background has been generated (*Grm1*^{tm1Dgen}, direct data submission to Mouse Genome Database (MGD), Deltagen and Lexicon Knockout Mice section, MGI, The Jackson Laboratory, Bar Harbor, Maine; http://www.informatics.jax.org/external/ko/). Interestingly, the main features associated to the neurologic phenotype and reported in *Grm1*^{tm1Dgen} homozygous animals are decreased body weight and length, and bone mineral density and content in mice at 49 days of age. The bone density defect reported in homozygous *Grm1*^{tm1Dgen} mice and the skeleton anomaly observed in *crv4*/*crv4* mice could represent the effects of a unique molecular mechanism. Variable expressivity of the bone phenotype between the two mouse mutants may be due to the different genetic backgrounds of the two animals. Both *crv4* and *Grm1*^{tm1Dgen} mouse skeletal observations could be related to recent evidence supporting a role of glutamate signalling in bone remodelling (32). Whilst functional glutamate signalling has been demonstrated in osteoblasts and osteoclasts *in vitro*, the effects of modulation of glutamate signalling *in vivo* are still unclear. The *crv4* mouse skeletal anomaly may be considered the first *in vivo* evidence that an impairment of glutamate pathway may be associated to a bone anomaly.

Functional clues of the pathophysiological processes involved in the *crv4* mouse phenotype anomalies could have a great significance in evaluating *in vivo* new and unknown functions of the *Grm1* gene in tissues different from nervous tissues.

Although no *Grm1* mutations have been reported so far as responsible for ataxia in hereditary forms of the disease, evidence indicates that the lack of a normal *Grm1* protein function because of auto-antibody production may be associated to ataxia in patients affected by Hodgkin's disease (33). Other evidence coming from the study of transgenic mouse models of SCA1 disorder (34) demonstrates the role of glutamate signalling as central to the normal functioning of cerebellum and indicates that alterations in glutamate signalling may play an important role in the pathophysiology of these neurological disorders. For all of these reasons, the study of *crv4* mice should help to unravel the pathogenetic mechanisms underlining neurological and associated phenotype anomalies.

Acknowledgements

We would like to thank our colleague Dominique Simon-Chazottes, Unité de Génétique fonctionnelle de la Souris, Institut Pasteur, Paris, for her kind help in the genetic mapping data analysis. This work was funded in part by a grant from the Italian Ministry of University (FIRB project) to R.R.

References

1. Bordi F and Ugolini A: Group I metabotropic glutamate receptors: implications for brain diseases. Prog Neurobiol 59: 55-79, 1999.
2. Pin JP and Duvoisin R: The metabotropic glutamate receptors: structure and functions. Neuropharmacology 34: 1-26, 1995.
3. Aronica E, Catania MV, Geurts J, Yankaya B and Troost D: Immunohistochemical localization of group I and II metabotropic glutamate receptors in control and amyotrophic lateral sclerosis human spinal cord: upregulation in reactive astrocytes. Neuroscience 105: 509-520, 2001.
4. Klockgether T and Evert B: Genes involved in hereditary ataxias. Trends Neurosci 21: 413-418, 1998.
5. Conquet F, Bashir ZI, Davies CH, *et al*: Motor deficit and impairment of synaptic plasticity in mice lacking mGluR1. Nature 372: 237-243, 1994.
6. Norreel JC, Jamon M, Riviere G, Passage E, Fontes M and Clarac F: Behavioural profiling of a murine Charcot-Marie-Tooth disease type 1A model. Eur J Neurosci 13: 1625-1634, 2001.
7. Jaubert J, Jaubert F, Martin N, *et al*: Three new allelic mouse mutations that cause skeletal overgrowth involve the natriuretic peptide receptor C gene (Npr3). Proc Natl Acad Sci USA 96: 10278-10283, 1999.
8. Ray K, Fan GF, Goldsmith PK and Spiegel AM: The carboxyl terminus of the human calcium receptor. Requirements for cell-surface expression and signal transduction. J Biol Chem 272: 31355-31361, 1997.
9. Ray K and Hauschild BC: Cys-140 is critical for metabotropic glutamate receptor-1 dimerization. J Biol Chem 275: 34245-34251, 2000.

10. Aiba A, Chen C, Herrup K, Rosenmund C, Stevens CF and Tonegawa S: Reduced hippocampal long-term potentiation and context-specific deficit in associative learning in mGluR1 mutant mice. Cell 79: 365-375, 1994.
11. Aiba A, Kano M, Chen C, *et al*: Deficient cerebellar long-term depression and impaired motor learning in mGluR1 mutant mice. Cell 79: 377-388, 1994.
12. Simonyi A, Xia J, Igbavboa U, Wood WG and Sun GY: Age differences in the expression of metabotropic glutamate receptor 1 and inositol 1,4,5-trisphosphate receptor in mouse cerebellum. Neurosci Lett 244: 29-32, 1998.
13. Cinque C, Zuena AR, Casolini P, *et al*: Reduced activity of hippocampal group-I metabotropic glutamate receptors in learning-prone rats. Neuroscience 122: 277-284, 2003.
14. Knopfel T and Grandes P: Metabotropic glutamate receptors in the cerebellum with a focus on their function in Purkinje cells. Cerebellum 1: 19-26, 2002.
15. Copeland NG, Hutchison KW and Jenkins NA: Excision of the DBA ecotropic provirus in dilute coat-color revertants of mice occurs by homologous recombination involving the viral LTRs. Cell 33: 379-387, 1983.
16. Stoye JP, Fenner S, Greenoak GE, Moran C and Coffin JM: Role of endogenous retroviruses as mutagens: the hairless mutation of mice. Cell 54: 383-391, 1988.
17. Seperack PK, Mercer JA, Strobel MC, Copeland NG and Jenkins NA: Retroviral sequences located within an intron of the dilute gene alter dilute expression in a tissue-specific manner. EMBO J 14: 2326-2332, 1995.
18. Druker R and Whitelaw E: Retrotransposon-derived elements in the mammalian genome: a potential source of disease. J Inherit Metab Dis 27: 319-330, 2004.
19. Jun K, Lee SB and Shin HS: Insertion of a retroviral solo long terminal repeat in mdr-3 locus disrupts mRNA splicing in mice. Mamm Genome 11: 843-848, 2000.
20. Sun H and Chasin LA: Multiple splicing defects in an intronic false exon. Mol Cell Biol 20: 6414-6425, 2000.
21. Kol G, Lev-Maor G and Ast G: Human-mouse comparative analysis reveals that branch-site plasticity contributes to splicing regulation. Hum Mol Genet, 2005.
22. Lam BJ and Hertel KJ: A general role for splicing enhancers in exon definition. RNA 8: 1233-1241, 2002.
23. Wang Z, Rolish ME, Yeo G, Tung V, Mawson M and Burge CB: Systematic identification and analysis of exonic splicing silencers. Cell 119: 831-845, 2004.
24. Cartegni L, Chew SL and Krainer AR: Listening to silence and understanding nonsense: exonic mutations that affect splicing. Nat Rev Genet 3: 285-298, 2002.
25. Blencowe BJ: Exonic splicing enhancers: mechanism of action, diversity and role in human genetic diseases. Trends Biochem Sci 25: 106-110, 2000.
26. Bailey JA, Liu G and Eichler EE: An Alu transposition model for the origin and expansion of human segmental duplications. Am J Hum Genet 73: 823-834, 2003.
27. Kang YK, Park JS, Lee CS, Yeom YI, Chung AS and Lee KK: Efficient integration of short interspersed element-flanked foreign DNA via homologous recombination. J Biol Chem 274: 36585-36591, 1999.
28. Cantrell MA, Filanoski BJ, Ingermann AR, *et al*: An ancient retrovirus-like element contains hot spots for SINE insertion. Genetics 158: 769-777, 2001.
29. Wilkinson MF: A new function for nonsense-mediated mRNA-decay factors. Trends Genet 21: 143-148, 2005.
30. Zhu H, Ryan K and Chen S: Cloning of novel splice variants of mouse mGluR1. Brain Res Mol Brain Res 73: 93-103, 1999.
31. Selkirk JV, Challiss RA, Rhodes A and McIlhinney RA: Characterization of an N-terminal secreted domain of the type-1 human metabotropic glutamate receptor produced by a mammalian cell line. J Neurochem 80: 346-353, 2002.
32. Mason DJ: Glutamate signalling and its potential application to tissue engineering of bone. Eur Cell Mater 7: 12-26, 2004.
33. Coesmans M, Smitt PA, Linden DJ, *et al*: Mechanisms underlying cerebellar motor deficits due to mGluR1-autoantibodies. Ann Neurol 53: 325-336, 2003.
34. Serra HG, Byam CE, Lande JD, Tousey SK, Zoghbi HY and Orr HT: Gene profiling links SCA1 pathophysiology to glutamate signaling in Purkinje cells of transgenic mice. Hum Mol Genet 13: 2535-2543, 2004.